

## INFLUENCE OF EXTRACTIVE REMOVAL ON TORREFACTION KINETICS OF PEQUI AGRO-EXTRACTIVE RESIDUES

Rafaela Barcelo <sup>a</sup>, Giulia Cruz Lamas <sup>a</sup>, Pedro Paulo O. Rodrigues <sup>a</sup>, Grace F. Ghesti <sup>b</sup>, Sandra Luz <sup>c</sup>, Patrick Rousset <sup>d</sup>, Edgar A. Silveira <sup>a\*</sup>

- a. University of Brasília, Mechanical Sciences Graduate Program, Laboratory of Energy and Environment, Brasília-DF, 70910-900, Brazil.
- b. University of Brasília, Chemistry Institute, Laboratory of Brewing Bioprocesses and Catalysis to Renewable Energy, Brasília, DF 70910-900, Brazil
- c. Faculty of Gama, University of Brasília, Brasília, DF 72444-240, Brazil
- d. French Agriculture Research Centre for International Development (CIRAD), 73 Rue J. F. Breton, 34398, Montpellier, Cedex 5, France

**ABSTRACT:** This work investigated the torrefaction process for waste-to-energy (WTE) of *Caryocar brasiliense* (pequi) seed. Torrefaction (mild pyrolysis) is a pretreatment process (220–300 °C) that improves raw biomass's chemical and physical properties. This investigation aims to understand the thermal degradation kinetics through the torrefaction of pequi seeds with (PS) and without extractives (PSWE) residues. The torrefaction was conducted in a micro-TGA at 220–260 °C; 7° C.min<sup>-1</sup> heating rate; and 60 min of holding time) was performed for PS and PSWE, characterizing their thermal behavior and providing data for the kinetic modeling. The higher extractive content of 40.73% resulted in a higher mass loss for PS, with solid yields of 78.30, 75.48 and 66.47%, while PSWE presented solid yields of 86.26, 77.79, and 66.71% considering 220, 240, and 260 °C treatments, respectively. The two-step reaction kinetics was applied and reported accurate results showing a suitable tool to predict the torrefaction kinetic ( $R^2 > 0.99$  for all predicted curves) of fruit seed with and without extractives. The results indicate that Light and Mild torrefaction are more influenced by extractive content on the raw biomass, with decomposition rate and final solid yield affected. Meanwhile, higher torrefaction severities showed that the decomposition rate is still superior for feedstock with extractives (PS), but the final solid yield is no more affected.

**Keywords:** torrefaction; extractives; seeds; biochar; modeling.

### 1 INTRODUCTION

The global environmental agenda has been focused on waste reduction, sustainable cities and recycling, and the recovery of valuable materials, primarily driven by strict disposal regulations, resource deficiencies, the adverse effects of global warming, and the significant increase in per capita waste production [1].

Thermochemical processes are increasingly being explored as Organic Waste-to-Energy (OWtE) technologies for converting solid organic wastes into valuable biofuels [2–5]. Among these processes, torrefaction is a promising technology that can overcome the inherent challenges associated with biomass.

Torrefaction is a mild-pyrolysis treatment conducted at 200 to 300 °C under an inert or oxygen-lean atmosphere to enhance biomass properties, such as higher energy density [6]. These desirable characteristics of torrefied biomass can significantly improve the efficiency of energy systems, reduce the cost of transportation, and optimize the management of residue valorization [7,8]. The torrefaction process has the potential to play a critical role in the development of sustainable and efficient energy systems for managing organic waste, thereby contributing to the circular economy and addressing the challenges associated with climate change [9].

The intricate morphological structure of *Caryocar brasiliense* (pequi fruit), characterized by numerous thorns and low grindability, makes it challenging to process and renders most pequi seeds (PS) as agro-industrial waste, causing significant environmental concerns that demand sustainable waste management alternatives [2]. Therefore, PS presents a promising feedstock for WTE.

Literature on pequi biomass mainly addressed its nutritional, pharmaceutical, and biodiesel applications

[10–19]. In addition, previous work assessed the valorization pathway of waste-to-energy (WTE) via pyrolysis, gasification, and transesterification of *Caryocar brasiliense* seeds to produce biochar, syngas, and biodiesel [3]. Different operating conditions were evaluated for the pyrolysis and gasification valuation routes of pequi seeds (PS), pequi seeds without extractives (PSWE), and their extractives, seeking the best combination and upgraded products. Exciting results were obtained for biodiesel production via transesterification after extractive removal [3]. Additionally, solid biofuel with enhanced energy properties was reported for PSWE compared to PS.

It was noted in the literature review that no studies had been conducted on the torrefaction treatment evaluating the thermal behavior and the influence of extractive removal on the degradation kinetics of PS and PSWE. Therefore, this work aims to further the previous investigation [2] by introducing the torrefaction route.

One of the methods used to investigate the kinetic mechanisms of biomass torrefaction is thermogravimetric analysis (TGA), which provides information on the thermal degradation behavior and the degradation rate. Furthermore, TGA is suitable as input data for modeling.

Determining torrefaction kinetics is essential for predicting the properties of biochar and designing reactors. The two-step kinetic model, first proposed by [20] and later explored [6,21–28], is reliable for accessing and predicting the thermal behavior of various biomass sources. In this context, the present work uses the two-step kinetic model to evaluate the influence of extractive removal on the torrefaction kinetics of pequi agro-extractive residues. Thus, it provides new insights into the valuation route of pequi residue. The results will assist in the development of small agro-food industries and reduce agro-residues' environmental impact on urban resource circularity.

## 2 MATERIAL AND METHODS

### 2.1 Feedstock

The feedstock applied in this study was the PS and PSWE residues. Feedstock preparation is illustrated in Fig. 1.

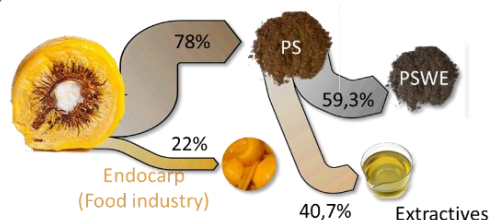


**Figure 1:** Feedstock preparation. Sankey diagram of mass percentage for pequi seed (PS) and pequi seed without extractives (PSWE).

The pequi fruit was sourced from the agro-industrial zone, composed of family farmers of the savanna biome (Emporium of Cerrado) in Goiás, central Brazil. The pequi fruit processing involves the removal of the pyrenes (pulp and seed) from the fibrous exocarp. The resulting endocarp, PS, can be separated after consuming the yellow edible pulp. In this study, PS was collected following proper pulp extraction and subjected to solvent extraction using ethanol in a Soxhlet system to obtain PSWE following the TAPPI Standards & Methods (T 204 om-88) with some modifications[2].

**Table I:** The proximate, lignocellulosic, ultimate, and calorific analysis for PS and PSWE raw material [2].

Feedstock[2]	PS	PSWE
<b>Proximate analysis (wt.%)</b>		
Ash	1.20	0.21
Fixed carbon	12.98	20.22
Volatile Matter	85.82	79.59
Moisture	25.32	0.00
<b>Ultimate analysis (wt.%)</b>		
C	55.09	50.07
H	8.11	7.82
N	1.29	1.21
O <sup>b</sup>	34.30	38.83
<b>Lignocellulosic analysis (wt%)</b>		
Holocellulose	60.65	68.18
Lignin	36.99	31.60
Extractives	40.73	0.00
<b>Calorific analysis</b>		
HHV (MJ kg <sup>-1</sup> ) <sup>c</sup>	22.69	21.06

<sup>a</sup> Dry basis, <sup>b</sup> by difference O = 100 - (C + H + N + ash), <sup>c</sup> calculated higher heating value[6].

Samples of 10 g of PS were subjected to solvent extraction for 24 hours, with the solvent being replaced every 6 hours[2]. The extractives were calculated by subtracting the weight of PSWE from that of PS[2]. Finally, PS and PSWE were oven-dried at 105 °C for 24 hours and ground in a mill with an 80–100 mesh size for further characterization[2]. Table I presents the characterization of raw feedstock provided by previous literature [2].

### 2.2 TGA apparatus and torrefaction procedure

The SDT Q600 TA thermogravimetric analyzer was applied to conduct PS and PSWE thermal degradation. The system comprises a gas control system (nitrogen

steel cylinder, a rotameter, N<sub>2</sub> flow of 50 mL min<sup>-1</sup>), a reaction unit, and a computer for system control and data collection and processing. Torrefaction was conducted in duplicate for temperatures of 220, 240, and 260 °C, with a holding time of 80 min and a heating rate of 7 °C min<sup>-1</sup>. The thermal degradation of the samples (5 mg, in alumina crucibles) was evaluated. The solid yield ( $S_Y$ ) over time was determined with Eq. (1)[21,28–30], providing the instantaneous mass variation (TGA).

$$S_Y^{(T)}(t) = \frac{m_i(t)}{m_0} \times 100 \quad (1)$$

Here,  $m_i$  is the solid mass during torrefaction,  $t$  is the residence time,  $m_0$  is the dried mass before torrefaction, and  $T$  the experiment temperature.

### 2.3 Kinetic modeling

The two-step kinetic model, firstly proposed by [20] and further optimized by [21,22], was applied to obtain kinetic reaction rates (solid ( $k_B$ ,  $k_C$ ) and volatile ( $k_{V_1}$ ,  $k_{V_2}$ )) and to predict the thermal degradation behavior. The model uses a first-order mechanism composed by a two-step consecutive reactions and four reaction rates constants  $k_i$  (min<sup>-1</sup>,  $i = B, C, V_1, V_2$ ) defined by the Arrhenius law [26]. In this approach, the torrefaction products are lumped into five pseudo-components: solid (feedstock  $A$ , intermediate solid  $B$  and residue  $C$ ) and volatiles  $V_1$  and  $V_2$ [20]. The total volatile is described by the sum of  $V_1$  and  $V_2$ . Meanwhile, the total solid yield is expressed by the sum of masses of  $A$ ,  $B$ , and  $C$ [20]. The model was applied by fitting numerical profiles to the experimental solid yield  $S_Y^{(T)}(t)$  (obtained with TG equipment) using a fmincon minimization function in Matlab® [26]. Detailed model can be accessed in previous publications [6,21–28].

## 3 RESULTS

### 3.1 Torrefaction

Figure 2 shows the TG curves of torrefaction treatments for PS and PSWE, highlighting the degradation behavior and solid yield differences.

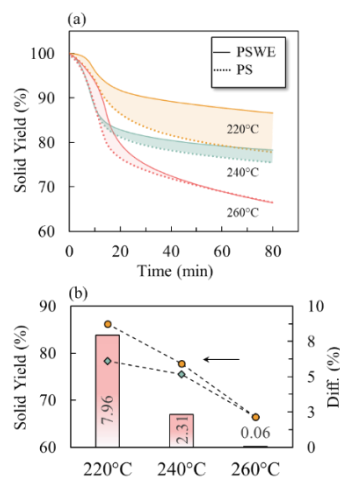


**Figure 2:** (a) TG curves of PS and PSWE for 220, 240, and 260 °C torrefaction. (b) Final  $S_Y$  differences for PS and PSWE.

The PS comprises the components of holocellulose, lignin, and extractives (vegetal fat)[2].The extractive compounds typically have lower molecular weights than the lignocellulosic components, making them more susceptible to thermal decomposition at lower temperatures[2]. As shown in Fig. 2(a), PS presented an earlier and pronounced mass loss for 220 and 240 °C compared to PSWE. The 260 °C treatment depicted a distinct and note behavior, where the decomposition rate of PS was faster than PSWE, but the final solid yield was nearly the same. The higher extractive content of 40.73% (Table I) resulted in a higher mass loss for PS, resulting in an  $S_Y$  of 78.30, 75.48, and 66.47%, while PSWE presented  $S_Y$  of 86.26, 77.79, and 66.71% considering 220, 240, and 260 °C treatments, respectively. Figure 2(b) elucidates this behavior showing a decrease in the final  $S_Y$  with increasing torrefaction temperature. The differences of final  $S_Y$  when comparing PSWE and PS were 7.96, 2.31, and 0.06% for 220, 240, and 260 °C, respectively.

3.2 Torrefaction kinetics

Figures 3 and 4 show the simulation results, displaying the experimental (dotted) versus numerically predicted curves (a) and the solid (b) and volatile (c) pseudo-components evolution during torrefaction treatment.

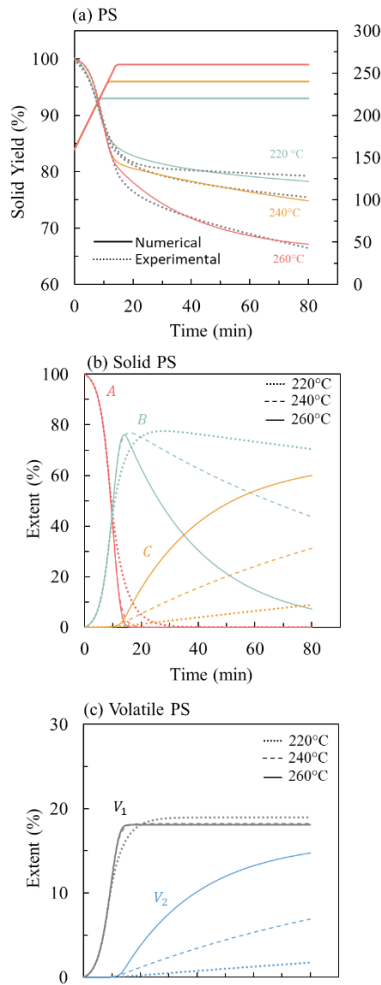


**Figure 3:** (a) Experimental and numerically predicted curves. The solid (b) and volatile (c) pseudocomponents evolve in time during torrefaction treatments of PS.

In addition, the Arrhenius plot of the kinetic rates obtained with predicted activation energies, pre-exponential factors and curve fit (Table II) is shown in Fig. 5, allowing a better interpretation of the competition rate between the occurring first ( $k_1$  and  $k_{V1}$ ) and second ( $k_2$  and  $k_{V2}$ ) step reactions.

The fitting between the predicted curves and the experimental data (Figs. 3(a) and 4(a)) validates the accuracy of two-step reaction modeling in predicting PS and PSWE thermal behavior during torrefaction. Furthermore, the numerical prediction (curve fit) resulted in an  $R^2$  of 0.9918, 0.9969, and 0.9980 for PS and 0.9913, 0.9976, and 0.9999 for PSWE, considering 220, 240, and 260 °C, respectively, showing, for instance, that the two-step reaction model is a reliable tool to describe the influence of extractive on the torrefaction kinetics.

The first step is mainly attributed to low molecular weight volatiles and moisture resulting essentially from hemicellulose thermal degradation. In parallel, the second step reaction is ascribed mainly to cellulose, the remaining hemicelluloses, and part of lignin degradation [31].

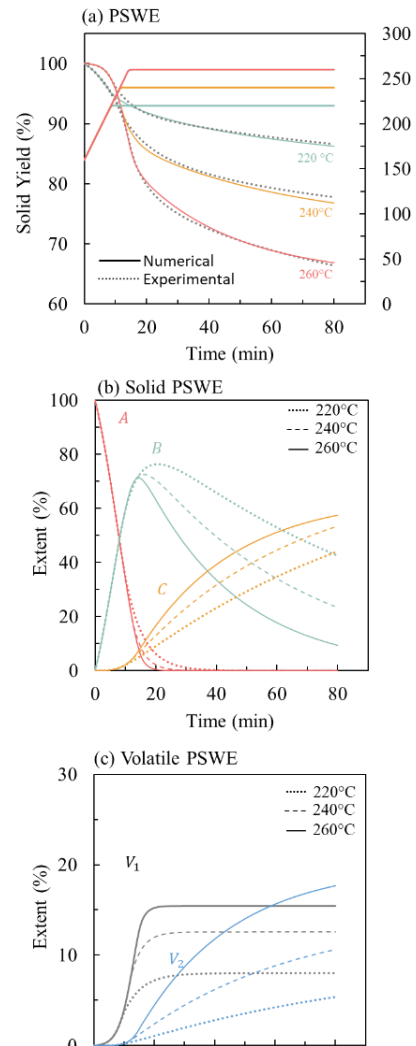


**Figure 4:** (a) Experimental and numerically predicted curves. The solid (b) and volatile (c) pseudo-components evolve in time during torrefaction treatments of PSWE.

As can be seen in Fig. 5, the ranking order shows a faster first-step reaction ( $k_1$  and  $k_{V_1}$ ) compared to the second-step ( $k_2$  and  $k_{V_2}$ ) for PS and PSWE, therefore presenting  $k_1 > k_{V_1} > k_2 > k_{V_2}$  for the torrefaction range between 220–260 °C. The resulting order of PS and PSWE kinetic rates can be interpreted by a stronger thermal cracking reaction and consequential greater releasing of volatiles. This behavior is not typical for wood biomass, which presents  $k_2 > k_{V_1}$  for lower torrefaction temperatures (200–230 °C), and when torrefaction severity increases, the  $k_{V_1}$  becomes more important than  $k_2$  [22].

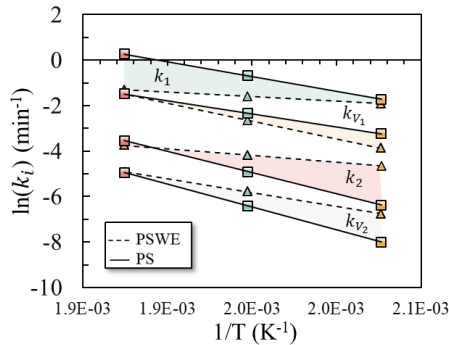


**Figure 5:** Arrhenius plot: calculated reaction rates competition.

A previous study evaluated the five fast-growth biomass plantations of Costa Rica concerning thermal degradation characteristics and devolatilization rate ( $D_{rate}$ ) using thermogravimetric analysis (TGA) [34]. The investigation established relationships between TGA parameters and  $D_{rate}$  with the contents of cellulose, lignin and extractives [34]. Furthermore, their results showed that a greater extractive content on biomass decreased the degradation temperatures of the different biomass components (hemicelluloses and cellulose) [34]. The previous statements align with the present investigation, where PS started its decompositions earlier and presented faster  $D_{rate}$  and pronounced mass loss (Figs. 3(a) and 4(a)). This behavior might be related to extractives presenting lower degradation temperatures than hemicellulose and cellulose [35] which, mixed, promoted thermal decomposition in earlier stages (temperatures and time) throughout torrefaction treatment.

Mészáros et al. [36] note that, during *Robinia pseudoacacia* (black locust) degradation, the devolatilization of extractives (mixed with the polymers in the wood) happens at two temperature ranges. The first occurs between 150–250 °C and is related to low molecular weight, while the second (between 250–550 °C) is linked to higher molecular weight [42].

As shown in Fig. 5, the first-step reaction ( $k_1$  and  $k_{V_1}$ ), mainly associated with hemicellulose degradation, presented faster reaction rates for PS than PSWE. The faster behavior of  $D_{rate}$  during the first-step reaction step can also be accessed by Figs. 3(b)(c) and Figs. 4(b)(c). The figures show a faster decomposition of pseudo-component A (before 20 min treatment) with a consequent fast formation of  $V_1$  for PS compared to PSWE. Another critical point is the extent of  $V_1$ , which was higher and nearly the same for the three torrefaction severities, considering PS torrefaction. Meanwhile, for PSWE, the release of  $V_1$  and its final extent% obeyed the

torrefaction severity, with faster  $D_{rate}$  and extent as severe the treatment. This faster  $D_{rate}$  on the first-step reaction might be attributed to extractives related to the first devolatilization stage (150–250 °C) before the devolatilization of hemicellulose occurs [34,36]. Those extractives generally correspond to the ones determined in hot or cold water (ASTM D-1110-84) [34].

The past investigation [34] also reported that the  $D_{rate}$  of cellulose was more affected by the extractives content than was  $D_{rate}$  of hemicellulose, indicating a higher degree of association of extractives with cellulose than hemicellulose. Regarding the second-step reaction of 220 and 240 °C torrefactions,  $k_2$  and  $k_{V_2}$  are faster for PSWE than PS, not highlighting the association of extractive with cellulose for those treatments. Nevertheless, considering 260 °C, the association is evident, with PS presenting a faster  $k_2$  reaction rate (Fig. 5). The association is also evident when evaluating the faster decomposition of B pseudo-component on Fig. 3(b). Therefore, in line with [36], which showed an association of the extractives relates to the second stage (250 to 550 °C) with wood cellulose compound. Those extractives generally correspond to the ones determined in hot water (ASTM D-1110-84) and NaOH (ASTM D-1109-84) [34].

The results could indicate, for instance, that Light and Mild torrefaction are more influenced by extractive content (association of extractive and hemicelluloses) on the raw biomass, affecting their decomposition rate and final solid yield. However, as torrefaction severity increases, the decomposition rate is still superior (due to the second stage of extractive release related to cellulose and extractive association) for feedstock with extractives (PS), but the final solid yield is no more affected.

**Table II:** Kinetic parameters (activation energy and pre-exponential factor) and curve fit quality ( $R^2$ ).

Reaction	Constant	$E_a i$	$A_o i$
<b>PS</b>			
$A \rightarrow B$	$k_1$	3.33E+04	4.98E+02
$A \rightarrow V_1$	$k_{V_1}$	1.31E+05	1.56E+12
$B \rightarrow C$	$k_2$	4.93E+04	1.62E+03
$B \rightarrow V_2$	$k_{V_2}$	1.02E+05	7.69E+07
<b>Curve fit</b>	220 °C	240 °C	260 °C
$R^2$	0.9918	0.9969	0.9980
<b>PSWE</b>			
$A \rightarrow B$	$k_1$	1.09E+05	6.49E+10
$A \rightarrow V_1$	$k_{V_1}$	9.55E+04	5.14E+08
$B \rightarrow C$	$k_2$	1.55E+05	4.67E+13
$B \rightarrow V_2$	$k_{V_2}$	1.67E+05	1.71E+14
<b>Curve fit</b>	220 °C	240 °C	260 °C
$R^2$	0.9913	0.9976	0.9999

$E_a i$ : Activation energy ( $J \cdot mol^{-1}$ )

$A_o i$ : pre-exponential factors ( $min^{-1}$ )

$i = 1, 2, V_1$  and  $V_2$

#### 4 CONCLUSIONS AND FUTURE DIRECTIONS

The present work evaluated the influence of extractive pequi seeds on torrefaction kinetics and final solid yield. The two-step reaction kinetics was applied and reported accurate results showing a suitable tool to

predict the torrefaction kinetic of fruit seed with and without extractives. The results indicate that Light and Mild torrefaction are more influenced by extractive content on the raw biomass, with decomposition rate and final solid yield affected. Meanwhile, higher torrefaction severities showed that the decomposition rate is still superior for feedstock with extractives (PS), but the final solid yield is no more affected. Such insight might promote research on biomass residues and is an asset for further research in other thermochemical valuation routes, such as gasification.

## 5 REFERENCES

- [1] L.N.B. Menezes, E.A. Silveira, J.V.S. Mazzoni, R.B.W. Evaristo, J.S. Rodrigues, G.C. Lamas, P.A.Z. Suarez, G.F. Ghesti, Alternative valuation pathways for primary, secondary, and tertiary sewage sludge: biochar and bio-oil production for sustainable energy, *Biomass Convers. Biorefinery*. (2022). <https://doi.org/10.1007/s13399-022-02543-9>.
- [2] G.F. Ghesti, E.A. Silveira, M.G. Guimarães, R.B.W.W. Evaristo, M. Costa, Towards a sustainable waste-to-energy pathway to pequi biomass residues: Biochar, syngas, and biodiesel analysis, *Waste Manag.* 143 (2022) 144–156. <https://doi.org/10.1016/j.wasman.2022.02.022>.
- [3] R.B.W. Evaristo, R. Ferreira, J. Petrocchi Rodrigues, J. Sabino Rodrigues, G.F. Ghesti, E.A. Silveira, M. Costa, Multiparameter-analysis of CO<sub>2</sub>/Steam-enhanced gasification and pyrolysis for syngas and biochar production from low-cost feedstock, *Energy Convers. Manag.* X. 12 (2021) 100138. <https://doi.org/10.1016/j.ecmx.2021.100138>.
- [4] M.C. Rodrigues, E.A. Silveira, A.C.P.B. Junior, On the correlation between thermal imagery and fugitive CH<sub>4</sub> emissions from MSW landfills, *Waste Manag.* 166 (2023) 163–170. <https://doi.org/10.1016/j.wasman.2023.05.005>.
- [5] G.C. Lamas, B. S. Chaves, P.P. Oliveira, T. Barbosa, T. da S. Gonzales, G.F. Ghesti, P. Rousset, E.A. Silveira, Effect of torrefaction on steam-enhanced co-gasification of an urban forest and landfill waste blend: H<sub>2</sub> production and CO<sub>2</sub> emissions mitigation, *Int. J. Hydrogen Energy*. (2023). <https://doi.org/https://doi.org/10.1016/j.ijhydene.2023.03.367>.
- [6] B.-J. Lin, E.A. Silveira, B. Colin, W.-H. Chen, A. Pétrissans, P. Rousset, M. Pétrissans, Prediction of higher heating values (HHVs) and energy yield during torrefaction via kinetics, *Energy Procedia*. 158 (2019) 111–116. <https://doi.org/10.1016/j.egypro.2019.01.054>.
- [7] W.-H. Chen, B.-J. Lin, Y.-Y. Lin, Y. Chu, A.T. Ubando, P.L. Show, H.C. Ong, J. Chang, S. Ho, A.B. Culaba, A. Pétrissans, M. Pétrissans, P. Loke, H. Chyuan, J. Chang, S. Ho, A.B. Culaba, A. Pétrissans, M. Pétrissans, Progress in biomass torrefaction: Principles, applications and challenges, *Prog. Energy Combust. Sci.* 82 (2021) 100887. <https://doi.org/10.1016/j.pecs.2020.100887>.
- [8] S.K. Thengane, K.S. Kung, A. Gomez-Barea, A.F. Ghoniem, Advances in biomass torrefaction: Parameters, models, reactors, applications, deployment, and market, *Prog. Energy Combust. Sci.* 93 (2022) 101040. <https://doi.org/10.1016/j.pecs.2022.101040>.
- [9] E. A. Silveira, B. Santanna Chaves, L. Macedo, G.F. Ghesti, R.B.W. Evaristo, G. Cruz Lamas, S.M. Luz, T. de P. Protásio, P. Rousset, A hybrid optimization approach towards energy recovery from torrefied waste blends, *Renew. Energy*. (2023). <https://doi.org/10.1016/j.renene.2023.05.053>.
- [10] H.P. Cornelio- Santiago, R.B. Bodini, A.L. Oliveira, Potential of Oilseeds Native to Amazon and Brazilian Cerrado Biomes: Benefits, Chemical and Functional Properties, and Extraction Methods, *J. Am. Oil Chem. Soc.* 98 (2021) 3–20. <https://doi.org/10.1002/aocs.12452>.
- [11] L.R.O. Torres, F.C. Santana, F.B. Shinagawa, J. Mancini-Filho, Bioactive compounds and functional potential of pequi (*Caryocar* spp.), a native brazilian fruit: A review, *Grasas y Aceites*. 69 (2018) 1–16. <https://doi.org/10.3989/gya.1222172>.
- [12] M.C. Lisboa, F.M.S. Wiltshire, A.T. Fricks, C. Dariva, F. Carrière, Á.S. Lima, C.M.F. Soares, Oleochemistry potential from Brazil northeastern exotic plants, *Biochimie*. 178 (2020) 96–104. <https://doi.org/10.1016/j.biochi.2020.09.002>.
- [13] R.C.M. dos Santos, P.C. Gurgel, N.S. Pereira, R.A. Breves, P.R.R. de Matos, L.P. Silva, M.J.A. Sales, R. de V.V. Lopes, Ethyl esters obtained from pequi and macaúba oils by transesterification with homogeneous acid catalysis, *Fuel*. 259 (2020) 116206. <https://doi.org/10.1016/j.fuel.2019.116206>.
- [14] E.N. Ferreira, T.B.M.G. Arruda, F.E.A. Rodrigues, D.T.D. Arruda, J.H. da Silva Júnior, D.L. Porto, N.M.P.S. Ricardo, Investigation of the thermal degradation of the biolubricant through TG-FTIR and characterization of the biodiesel – Pequi (*Caryocar brasiliensis*) as energetic raw material, *Fuel*. 245 (2019) 398–405. <https://doi.org/10.1016/j.fuel.2019.02.006>.
- [15] C.M. Marques Cardoso, D.G. Zavariz, G.E. Gama Vieira, Transesterification of Pequi (*Caryocar brasiliensis* Camb.) bio-oil via heterogeneous acid catalysis: Catalyst preparation, process optimization and kinetics, *Ind. Crops Prod.* 139 (2019) 111485. <https://doi.org/10.1016/j.indcrop.2019.111485>.
- [16] T.A. Silva, R.M.N. De Assunção, A.T. Vieira, M.F. De Oliveira, A.C.F. Batista, Methyl and ethylic biodiesels from pequi oil (*Caryocar brasiliense* Camb.): Production and thermogravimetric studies, *Fuel*. 136 (2014) 10–18. <https://doi.org/10.1016/j.fuel.2014.07.035>.
- [17] P.A. Cremonez, M. Feroldi, C. de Jesus de Oliveira, J.G. Teleken, T.W. Meier, J. Dieter, S.C. Sampaio, D. Borsatto, Oxidative stability of biodiesel blends derived from different fatty materials, *Ind. Crops Prod.* 89 (2016) 135–140. <https://doi.org/10.1016/j.indcrop.2016.05.004>.
- [18] M.R. da S. Miranda, C.A.G. Veras, G.F. Ghesti, Charcoal production from waste pequi seeds for heat and power generation, *Waste Manag.* 103 (2020) 177–186. <https://doi.org/10.1016/j.wasman.2019.12.025>.

- [19] A.L. Macedo, R.S. Santos, L. Pantoja, A.S. Santos, Pequi cake composition, hydrolysis and fermentation to bioethanol, *Brazilian J. Chem. Eng.* 28 (2011) 9–15. <https://doi.org/10.1590/S0104-66322011000100002>.
- [20] C. Di Blasi, M. Lanzetta, Intrinsic kinetics of isothermal xylan degradation in inert atmosphere, *J. Anal. Appl. Pyrolysis*. 40–41 (1997) 287–303. [https://doi.org/10.1016/S0165-2370\(97\)00028-4](https://doi.org/10.1016/S0165-2370(97)00028-4).
- [21] B.-J. Lin, E.A. Silveira, B. Colin, W.-H. Chen, Y.-Y. Lin, F. Leconte, A. Pétrissans, P. Rousset, M. Pétrissans, Modeling and prediction of devolatilization and elemental composition of wood during mild pyrolysis in a pilot-scale reactor, *Ind. Crops Prod.* 131 (2019) 357–370. <https://doi.org/10.1016/j.indcrop.2019.01.065>.
- [22] E.A. Silveira, S.M. Luz, R.M. Leão, P. Rousset, A. Caldeira-Pires, Numerical modeling and experimental assessment of sustainable woody biomass torrefaction via coupled TG-FTIR, *Biomass and Bioenergy*. 146 (2021). <https://doi.org/10.1016/j.biombioe.2021.105981>.
- [23] E.A. Silveira, M.S. Santanna, N.P. Barbosa Souto, G.C. Lamas, L.G.O. Galvão, S.M. Luz, A. Caldeira-Pires, Urban lignocellulosic waste as biofuel: thermal improvement and torrefaction kinetics, *J. Therm. Anal. Calorim.* 148 (2023) 197–212. <https://doi.org/10.1007/s10973-022-11515-0>.
- [24] E.A. Silveira, L.G. Oliveira Galvão, L. Alves de Macedo, I. A. Sá, B. S. Chaves, M.V. Girão de Morais, P. Rousset, A. Caldeira-Pires, Thermo-Acoustic Catalytic Effect on Oxidizing Woody Torrefaction, *Processes*. 8 (2020) 1361. <https://doi.org/10.3390/pr8111361>.
- [25] L.G.O.B.S.C. Galvão, M.V.G. de Morais, A.T. do V. Vale, A. Caldeira-Pires, P. Rousset, E.A. Silveira, Combined thermo-acoustic upgrading of solid fuel: experimental and numerical investigation, 28th Eur. Biomass Conf. Exhib. (2020) 6–9. <https://doi.org/10.5071/28thEUBCE2020-3DO.6.2>.
- [26] E.A. Silveira, B.J. Lin, B. Colin, M. Chaouch, A. Pétrissans, P. Rousset, W.H. Chen, M. Pétrissans, Heat treatment kinetics using three-stage approach for sustainable wood material production, *Ind. Crops Prod.* 124 (2018) 563–571. <https://doi.org/10.1016/j.indcrop.2018.07.045>.
- [27] E.A. Silveira, L. Macedo, P. Rousset, J.-M. Commandré, L.G.O. Galvão, B.S. Chaves, The effect of potassium carbonate wood impregnation on torrefaction kinetics, in: 29th Eur. Biomass Conf. Exhib., 2021. <https://doi.org/10.5071/29thEUBCE2021-3DV.6.4>.
- [28] B. Lin, E.A. Silveira, B. Colin, M. Chaouch, A. Pétrissans, P. Rousset, M. Pétrissans, Experimental and numerical analysis of poplar thermodegradation, in: V.M. and E. Hein (Ed.), 6th Int. Sci. Conf. Hardwood Process., Natural Resources Institute Finland, Helsinki, 2017: pp. 319–325. <http://urn.fi/URN:ISBN:978-952-326-509-7>.
- [29] E.A. Silveira, M.V.G. de Morais, P. Rousset, A. Caldeira-Pires, A. Pétrissans, L.G.O. Galvão, Coupling of an acoustic emissions system to a laboratory torrefaction reactor, *J. Anal. Appl. Pyrolysis*. 129 (2018) 29–36. <https://doi.org/10.1016/j.jaap.2017.12.008>.
- [30] E.A. Silveira, B. Lin, B. Colin, A. Pétrissans, P. Rousset, Mathematical approach to build a numerical tool for mass loss prediction during wood torrefaction, in: Veikko Möttönen and Emilia Heinonen (Ed.), 6th Int. Sci. Conf. Hardwood Process., Natural Resources Institute Finland (Luke), Helsinki, 2017: pp. 272–279. <http://urn.fi/URN:ISBN:978-952-326-509-7>.
- [31] E.A. Silveira, L.A. Macedo, P. Rousset, K. Candelier, L.G.O. Galvão, B.S. Chaves, J.-M. Commandré, A potassium responsive numerical path to model catalytic torrefaction kinetics, *Energy*. 239 (2022) 122208. <https://doi.org/10.1016/j.energy.2021.122208>.
- [32] Q.-V. Bach, T.N. Trinh, K.-Q. Tran, N.B.D. Thi, Pyrolysis characteristics and kinetics of biomass torrefied in various atmospheres, *Energy Convers. Manag.* 141 (2017) 72–78. <https://doi.org/10.1016/j.enconman.2016.04.097>.
- [33] R.B. Bates, A.F. Ghoniem, Biomass torrefaction: Modeling of volatile and solid product evolution kinetics, *Bioresour. Technol.* 124 (2012) 460–469. <https://doi.org/10.1016/j.biortech.2012.07.018>.
- [34] R. Moya, A. Rodríguez-Zúñiga, A. Puente-Urbina, Thermogravimetric and devolatilisation analysis for five plantation species: Effect of extractives, ash compositions, chemical compositions and energy parameters, *Thermochim. Acta.* 647 (2017) 36–46. <https://doi.org/10.1016/j.tca.2016.11.014>.
- [35] T. Sebio-Puñal, S. Naya, J. López-Beceiro, J. Tarrío-Saavedra, R. Artiaga, Thermogravimetric analysis of wood, holocellulose, and lignin from five wood species, *J. Therm. Anal. Calorim.* 109 (2012) 1163–1167. <https://doi.org/10.1007/s10973-011-2133-1>.
- [36] E. Mészáros, E. Jakab, G. Várhegyi, TG/MS, Py-GC/MS and THM-GC/MS study of the composition and thermal behavior of extractive components of Robinia pseudoacacia, *J. Anal. Appl. Pyrolysis*. 79 (2007) 61–70. <https://doi.org/10.1016/j.jaap.2006.12.007>.
- [37] M. Chai, L. Xie, X. Yu, X. Zhang, Y. Yang, M.M. Rahman, P.H. Blanco, R. Liu, A. V. Bridgwater, J. Cai, Poplar wood torrefaction: Kinetics, thermochemistry and implications, *Renew. Sustain. Energy Rev.* 143 (2021). <https://doi.org/10.1016/j.rser.2021.110962>.

## 6 ACKNOWLEDGEMENTS

The research presented was supported by Brazilian National Council for Scientific and Technological Development (CNPq), DPI/UnB, Brazilian Forest Products Laboratory (LPF), and the Federal District Research Foundation (FAPDF – Fundação de Apoio à Pesquisa do Distrito Federal, Edital 3/2021 – Project 00193.00000756/2021-35) for the financial support.

## 7 LOGO SPACE

